D. PAULRAJ[1], P.D. JEYAKUMAR[1*], G. RAJAMURUGAN[2], P. KRISHNASAMY[2]

INFLUENCE OF NANO TiO2/MICRO (SiC/B4C) REINFORCEMENT ON THE MECHANICAL, WEAR AND CORROSION BEHAVIOUR OF A356 METAL MATRIX COMPOSITE

This work investigates the distribution and the effect of synthesized nano TiO_2, micro SiC and B_4C particle on the aluminium (A356) metal matrix composites (AMMC). The consequences of this reinforcement on the mechanical, tribology and corrosion behaviour of the AMMC matrix are analyzed. The nano TiO_2 is synthesized by wet chemistry sol-gel process, and the reinforcements are added with A-356 by stir casting method. The ASTM standard test specimens are characterized through mechanical, tribology, and corrosion tests for identifying their properties. The metallurgical characterization has been deliberated through XRD and SEM with EDS. In the tensile test results, the percentage of elongation is dropped drastically by 73% due to the enhanced volume % of nano TiO_2, micro SiC, and B_4C particles. The particle addition of the wear rate and weight loss are reduced at different volume percentages of the A356 matrix. The time plays a significant role in the corrosion rate. The test results also confirm that the corrosion rate is comparatively minimum in 24 hrs (592.35 mm/yr) duration than the 48 hrs (646.368 mm/yr) in both the solutions.

Keywords: Nano TiO_2, SiC; B_4C, Wear, Corrosion

1. Introduction

Composite materials have more attractive properties like robustness and lightweight than traditional materials. MMCs are preferred for various engineering applications, especially in the automotive sector, to meet the various standard and customer requirements [1-2]. The multiple properties of the MMCs are improved by incorporating the different type and percentage (volume and weight) of the reinforcement in the matrix [3]. The effective distribution of the reinforcement in the base metal and the interfacial integrity will describe composite material properties. During the reinforcement synthesis process, structural and chemical integrity will not be disturbed [4-6]. MMC usage is preferred for structural applications in the automotive and aerospace industries by considering the lightweight and high strength. Due to the better corrosion resistance and wear resistance qualities have extended their usage in new areas such as shipbuilding and military applications [7]. Even though high abundance, aluminum usage is very limited in all sectors due to the soft and low hardness. In this manner, the researchers are tremendously working to increase the metals required properties.

The aluminium metal matrix composite is used in the automotive sector to manufacture vehicle components like engine piston, block, crankcase, and brake components [8-10]. The Al-Si will have a higher affinity to seizure and scuffing makes nearer to the boundary. Researchers have attempted to resolve these problems by adding solid lubricants like graphite and good results in resisting the above problems [11-12]. The different volume fraction of nano- Al_2O_3 has improved the tensile, yield strength, and ductility with an effective blend with the aluminium matrix [13]. The increased volume fraction of coated B_4C particles will lead to agglomeration of the particles and porosity [14]. The improvements of tensile strength, elongation, and toughness have improved by maintaining the optimum volume of reinforcement in the matrix [15-16]. The ceramics particles like glass, SiC, B_4C, Si_3N_4, B_4C, TiB_2, Al_2O_3, SiO_2, fly ash are reinforced with an aluminium matrix, which enriches the wear resistance [17-18].

The weight reduction of the composite is achieved by reducing the density, among which lithium has a higher solubility in aluminium. In addition to that, it provides an excellent response to age hardening [19]. The heat treatment bath will enhance the impact strength and corrosion resistance [20]. The magnesium-aluminum alloys corrosion rate particulates with TiC composite material in the sodium chloride solution and shows a lower value than the base matrix [20-21]. The metal matrix composites (MMC) are commonly embraced to replace

1   B.S. ABDUR RAHMAN CRESCENT INSTITUTE OF SCIENCE AND TECHNOLOGY, DEPARTMENT OF MECHANICAL ENGINEERING, CHENNAI-600 048, TAMILNADU, INDIA
2   VELLORE INSTITUTE OF TECHNOLOGY, SCHOOL OF MECHANICAL ENGINEERING, VELLORE-632014, TAMILNADU, INDIA

*   Corresponding author: pdjeyakumar@gmail.com

872

conventional material almost in all automobile areas. To improve the composite materials performance, the reinforcement type, size of the particle, and distribution particle in the matrix play a crucial role in the fabrication of MMCs. Much research was carried out on particulate reinforcement of MMCs; however, most of this work has focused on Nano-micro-metric particle dispersions. The production and use of micro-metric dispersion strengthened aluminum composite can significantly increase their physical and chemical properties.

In this work, the authors are fascinated to investigate the distribution and the effect of synthesized nano TiO_2, SiC, and B_4C particles on the aluminium (A356) metal matrix composites (AMMC). The impact of these reinforcements on the mechanical, tribology, and corrosion behaviour are analyzed through tensile, hardness, impact, tribology, and corrosion test. The metallurgical characterization has been reflected through SEM.

2. Experimental Details

2.1. Materials and Fabrication

The aluminium (A356) is procured from the indigenous Pvt Ltd Chennai. The chemical composition and the mechanical properties of A356 are found in Table 1 and Table 2, respectively. The titanium isopropoxide, ethanol, and cetyl trimethyl ammonium bromide have bought from Sigma-Aldrich. The 99.0% purity analytical grades of chemicals are utilized for this investigation. The fabricated AMMC specimen work plan is shown in Fig. 1.

TABLE 1

Chemical composition of Aluminium alloy A356 (in wt %)

% Element	Si	Fe	Cu	Mn	Mg	Zn	Ti	Al
Minimum	6.5	—	—	—	0.2	—	—	
Maximum	7.5	0.6	0.25	0.35	0.48	0.35	0.25	Bal.
Actual	7.1	0.22	0.04	0.12	0.45	0.02	0.1	

TABLE 2

Properties of Aluminium (A356)

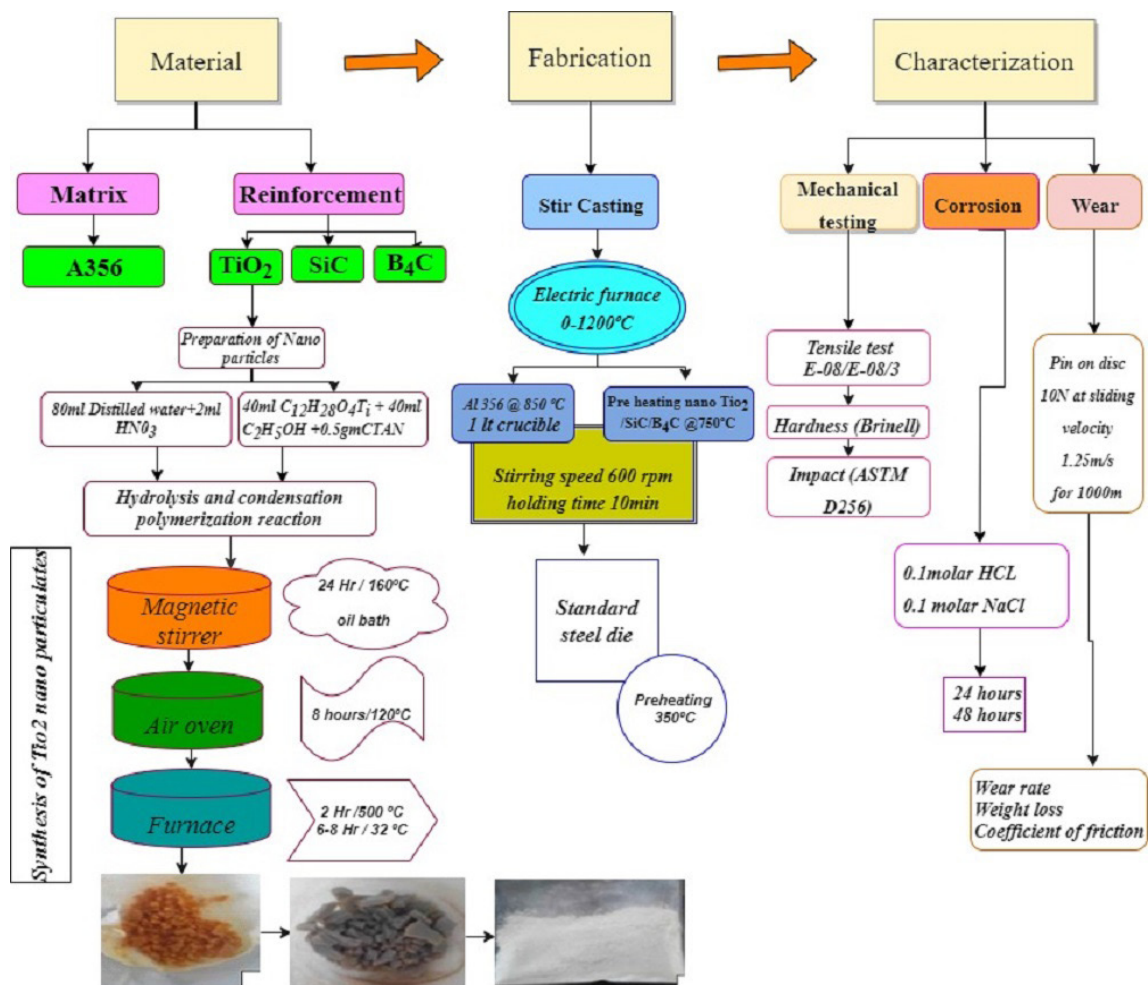| Sl. No.	Properties	Al
	Ultimate Tensile Strength (MPa)	110
	Young's Modulus E (GPa)	71
	Density(g/cm^3)	2.78
	Poisson's Ratio	0.33
	Elongation (%)	43
	Coefficient of Thermal Expansion ($\times 10^{-6}$ m/m K)	22.2
	Melting Point (°C)	730

Fig. 1. Work plan

2.1.1. Reinforcements

Three reinforcement particles (TiO$_2$, SiC, and B$_4$C) are identified to fabricate AMMC composite specimens. The reinforcement powders were procuded from Sigma-Aldrich India limited, Banglore. Subsequently, the synthesized TiO$_2$ nano particle (100 nm), and the other two particles (SiC and B$_4$C) are added in the micro size (10 μm). The respective volume percentages (0.5, 5, and 10%) of these nano and microparticles are used and preferred to fabricate AMMC specimens

2.1.2. Synthesis of nano TiO$_2$

An erstwhile used Sol-gel process synthesizes the nano titanium dioxide. In a typical procedure, 80 ml of distilled water is mixed with 2 ml of concentrated HNO$_3$. Another beaker with 40 ml of titanium isopropoxide (C$_{12}$H$_{28}$O$_4$Ti) and 40 ml of ethanol (C$_2$H$_5$OH) is adequately mixed, and 0.5g of Cetyl Trimethyl Ammonium Bromide (CTAB) is added into the beaker. The mixed contents undergo hydrolysis and condensation polymerization reaction to get the gel. The procedure is continued until the formation of a milky solution. The mixture is stirred for 24 hours at a constant temperature of 160°C±5°C, using a hot oil

bath. The obtained content is filtered and allowed to dry for about 8 hrs in a hot air oven at 120°C. The photographic image of water dried precursor has shown in Fig. 2a. This content is placed in a furnace for calcination at 500°C for 2 hours and allow to dry for about 6-8 hrs. The dried calcinated precursor photographic image is shown in Fig. 2b. This precursor is ground in a ball mill, and the final product is obtained in powder form, which has demonstrated in Fig. 2c. The X-Ray diffraction is a tool for identifying whether a material has an amorphous structure or crystalline structure. The synthesized nano TiO$_2$ is analyzed, and a graph is plotted between 2θ and intensity, which represents the nano powder's peak values compared with the standard PDF chart. The 2θ peak values of 25, 48, and 55 (Fig. 3) represent a crystalline phase present in their structure, and this value is matched with an existing JCPDS software graph. The graph peak corresponding to TiO$_2$ is confirmed using the d – spacing values from the software's PDF files. From the PDF 89-4921 and 89-8304, it was confirmed that the samples was TiO$_2$.

2.1.3. Fabrication of AMMCs specimen

The AMMC specimens are synthesized by the stir casting method. In the fabrication of AMMC, the A356 is weighted.
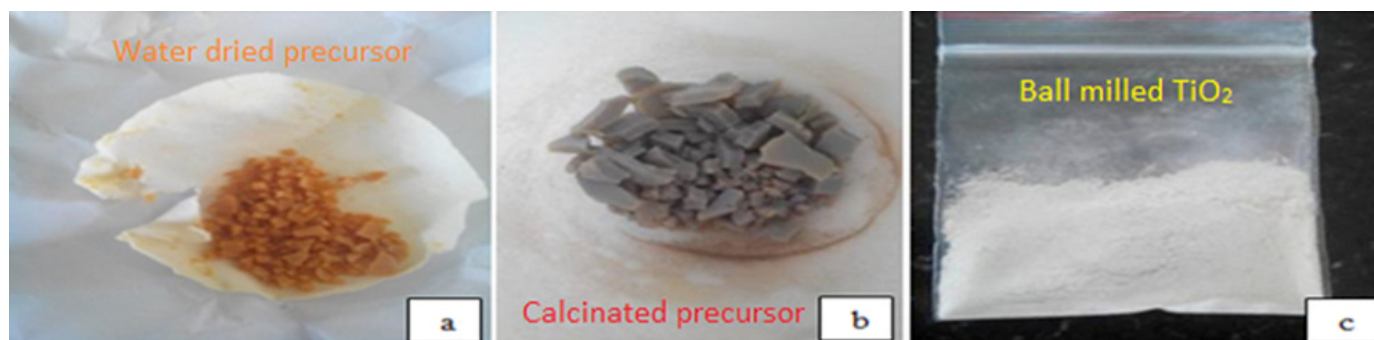

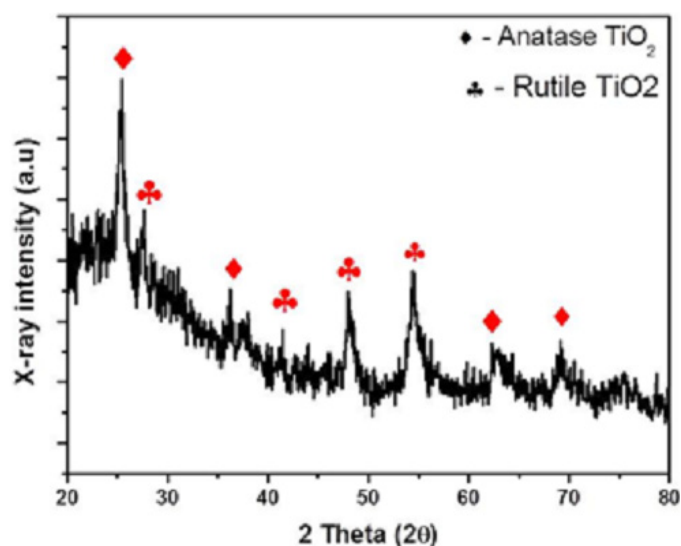Fig. 2. Photographic image of synthesized nano TiO$_2$ particle

Fig. 3. XRD Spectrum of TiO$_2$ nano powder

It is collected in the graphite crucible of capacity 1 liter, kept in an electric resistance furnace, and heated up to 850°C to get the molten A356 matrix. The preheated nano TiO$_2$ (nTiO$_2$), micro SiC and B$_4$C particles are mixed (Table 3) on the molten A356

TABLE 3

Different proportions of matrix and reinforcements

Type of composites	The volume percentage of the AA356 matrix	The volume percentage of reinforcement particle		
		Nano TiO$_2$	Micro SiC	Micro B$_4$C
AMMC1	100	0	0	0
AMMC2	94.5	0.5	5	0
AMMC3	89	1	10	0
AMMC4	94.5	0.5	0	5
AMMC5	89	1	0	10
AMMC6	79	1	10	10

874

matrix with a stirring speed 600 rpm. The process parameters for the fabrication of AMMC are presented in Table 4. Finally, the molten mixture is poured into a preheated ASTM standard steel die and allowed for solidification.

TABLE 4

Parameters/conditions of MMC fabrication

Conditions	Parameters/ Materials	Reference
Pouring temperature (°C)	800	[10,21,24,26,27]
Preheating temperature of reinforcement (°C)	750	[24,26]
Stirring speed (rpm)	600	[21,26]
Holding time (min)	10	[21,26]
Crucible type	Graphite	[10, 21, 22,26]
Mould material	Alloy steel	[24,26]
Mould preheating temperature (°C)	350	[21,26]

2.2. Mechanical testing

2.2.1. Tensile test

The stir cast composite specimens are subjected to a tensile test according to the ASTM E-08/E-08M standard. The Instron 3369 Universal Testing Machine is used to perform the tensile test. The tensile test specimens are positioned vertically in the upper and lower fixtures. The fixture's relative motion calculates the testing speed, and the crosshead is 1.27 mm/min. The results are obtained by the mean of six AMMCs tensile specimens, and the ultimate tensile strength and percentage of elongation have been measured during the test.

2.2.2. Hardness test

The developed AMMC composite's surface property in terms of hardness value is assessed through ϕ5 mm steel ball indenter on Brinell hardness testing machine. The specimens are polished up to 1μm surface finish, and the hardness test is conducted at three locations with a constant load of 500 Kg. The results are tabulated from the mean value of six AMMC specimens at various locations.

2.2.3. Impact test

The Impact strength of the stir cast AMMC composite specimens is tested based on ASTM-D256. The impact testing machine is used to carry out the testing, and the machine has a dimension of $600 \times 390 \times 600$ mm^3 with a pendulum weight of 64 kg with a 0.001 J resolution. The Izod specimens are prepared with the dimensions of $10 \times 10 \times 75$ mm and the notch angle of 45° with 2mm deep and 0.25 mm root radius. The test

specimen is positioned vertically at the testing machine's grips in front of a heavy swinging pendulum. The pendulum is released and allowed to strike through the specimen. The mean impact strength of six AMMC specimens is recorded for further analysis.

2.3. Wear test

The AMMC composite specimens' tribological properties are analyzed using Ducom Wear Tester-TR-201 CL wear and friction monitor, India (pin-on-disc machine).The device was integrated with a personal computer with a data acquirement system. The wear test is performed under dry sliding conditions at 25°C against AISI D2 high carbon-high chromium steel disc with 65 HRC. The applied load of 10 N at a sliding velocity of 1.25 m/s (400 rpm) for a 1000 m sliding distance is preferred to accomplish the test as per the ASTM G 99-05. The specimens' weight loss due to the sliding wear was determined by an electronic weighing balance (Shimadzu-AUW220D) with an accuracy of 0.001 mg.

2.4. Corrosion test

The solution immersion test is carried out to estimate the corrosion behaviour of AMMC specimens. The two different solutions of 0.1 molar of HCl and 0.1 molars of NaCl are prepared for the solution immersion test. The acid solution is prepared for 1 liter, in that 1/4th is an acid solution, and the remaining 3/4th is water. The acid solution is prepared with 0.5%, 1%, 1.5% and 2% concentrations. These acid solutions are mixed with distilled water so that no minerals will react in that specimen. The AMMC corrosion test specimens are prepared with 10 mm length and 10 mm diameter. The AMMC specimens are polished with 120-grade emery paper. 50 ml of HCl and NaCl conducts the corrosion test in a 100 ml beaker. Each specimen's initial weight is calculated before immersing the specimens into the 24 and 48 hrs immersion solution test. Consequently, the specimens are washed with distilled water and kept in a hot air oven at about 100°C for 1 hour to remove the moisture content. Similarly, each specimen's weight is estimated, and the percentage of corrosion is determined. The following mathematical relation is used to calculate the prepared AMMC specimens' corrosion rate.

$$Corrosion\ rate = 86.6\ X \left(\frac{W}{DAT} \right)\ mm/yr \qquad (1)$$

The weight loss (W) mg, density (D) g/cm^3, area of the specimen (A) cm^2, and the exposure time of the AMMC specimen (T) in hours are considered for estimating the corrosion rate.

2.5. Metallurgical studies

The SEM and optical microscope are used to examine AMMC specimens' microstructure after the sliding wear and

fracture. The specimens are polished with four different grade emery sheets and finally etched with Keller's etchant. The SEM images are captured with an accelerating voltage of 15 kV using SEM (Hitachi S–3000H) scanning electron microscope. The SEM test with EDS study is conducted under high vacuum with 20 kV voltages for tensile test and 30 kV for corrosion test. The composite surface is polished with a micro polisher and etched with an HF solution before characterization.

3. Results and discussion

3.1. Mechanical properties

The synthesized different percentages of particle reinforced AMMC1-6 specimens are subjected to the tensile test, and the obtained results are presented in Fig. 4. The presence of nano-TiO_2, SiC, and B_4C particles in A346 increases the grain boundary area, and it is due to the occupation of the intermediate position of nano and microparticles. Moreover, the nanoparticle nucleates into the structure of AMMC and form several fine grains during its solidification process compared with pure aluminium material. This fine grain boundary opposes the cup and cone fracture during the tensile test. Good brittle fracture has been seen due to the barrier of dislocation of aluminium to form a hard precipitate of nano particulates that act as the strengthening medium. Therefore, the tensile strength increase is directly proportional to the reinforcement content. The tensile strength is enhanced by 9.41% by increasing the nano TiO_2 from 0.5% to 1% along with SiC (5% to 10%) in AMMC2 and AMMC3. Similarly, the increase of nanoTiO_2 from 0.5% to 1% and B_4C (5% to 10%) improves the tensile strength by about 9.11%. At the volume percentage of 1% (nanoTiO_2), 10% SiC, and 10% B_4C the maximum tensile strength is observed at about 38.33% compared to AMMC1.

In the evaluation of the percentage of elongation, it was observed that the percentage of elongation decreased drastically by 73% (Fig. 5) due to the volume percentage of nano TiO_2 (1%), micro SiC (10%), and B_4C (10%) particles. The AMMC1 shows cup and cone fracture elongation, but reinforcement particles' influence reduces elongation and shows very low and brittle fracture elongation.
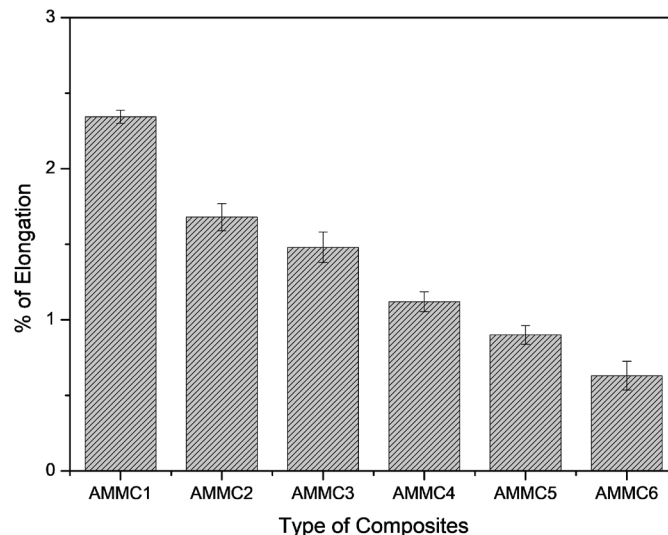

Fig. 5. Elongation of various composite specimens

The hardness of the fabricated AMMC is increased due to the addition of nano TiO_2, SiC, and B_4C. The increase in the volume fraction of the reinforcement particles increases their total surface resistance on the metal matrix composite. The A356 matrix forms the reinforcement strain zone around the nanoparticles because the thermal expansion leads to improve the hardness of AMMCs (Fig. 6). The AMMCs containing nanomaterial shows the enhanced value of hardness strength; this may be due to the presence of different micro reinforcement in the fabricated composites.

The obtained Izod impact test result was shown in Fig. 7. It figures revealed that the impact strength decreases with increasing the volume percentage of reinforcement particles.
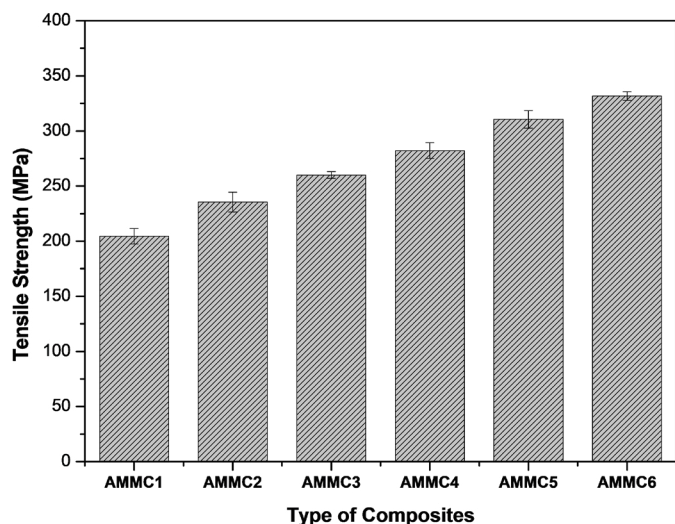

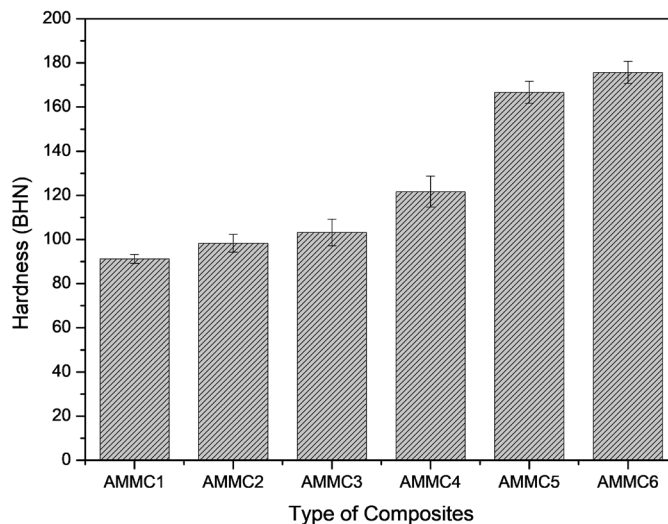Fig. 4. Tensile strength of different composites

Fig. 6. Hardness value of various composite specimens

876

The increased impact energy may attribute due to the grain boundary pinning of nanoparticulate over the A356 material. It may lead to the structural orientation and modification, which results in a decrease in the impact energy (Fig. 7). This result reveals a significant reduction in the impact strength of AMMC6 with 63.25% compared to the AMMC1 material.
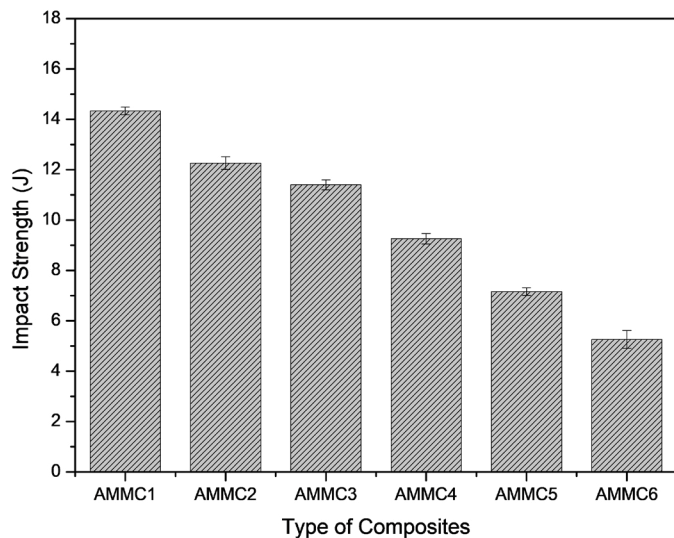

Fig. 7. Impact strength of various composite specimens

3.2. Wear performance

The obtained wear result reveals that the AMMC1 specimen undergoes prominent abrasive wear during dry sliding because of its soft nature [7]. The specimen allows deep groves and causing extensive plastic deformation over the pin surface, leading to more material loss and more wear rate. The embedded nano and micro reinforcement materials sustain the contact surface quality, prevent plastic deformation, and minimize the contact surfaces' abrasion. A minimum amount of worn debris is developed on the contact surface. The generations of cavities are found due to the delamination and tearing of the surface material. The presence of nano TiO_2, SiC, and B_4C reinforcement are distracted the smooth sliding of the pin over the disc. In AMMC3 composite, the weight loss is drastically reduced up to 27.77% due to the influence of nano TiO_2 (1%) and SiC (10%) compare to the base material (Fig. 8). Subsequently, the wear resistance is enriched by 38.88% with the maximum reinforcement of 1% TiO_2 + 10% SiC + 10% B_4C (AMMC6) compared to A356 (Fig. 8 and Fig. 9). It may primarily due to the influence of the B_4C particle induce the porosity in the specimen.

The experiment results show that the high coefficient of friction obtained by the nano TiO_2, SiC, and B_4C reinforced metal matrix composites compared with the base matrix. The frictional coefficient's effect falls for the different volume percentages of particle addition into the composite matrix. According to the particles' appropriate addition, the introduction of the nano TiO_2 particles enhances the resistance towards abrasion and gradual increment in the friction co-efficient properties (Fig. 10).
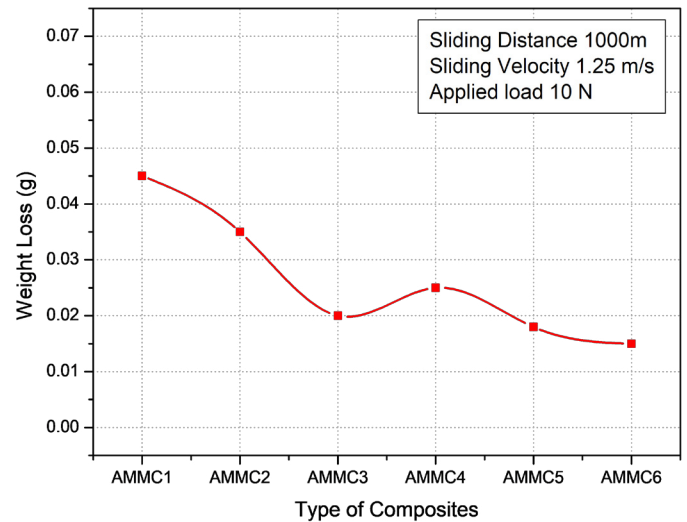

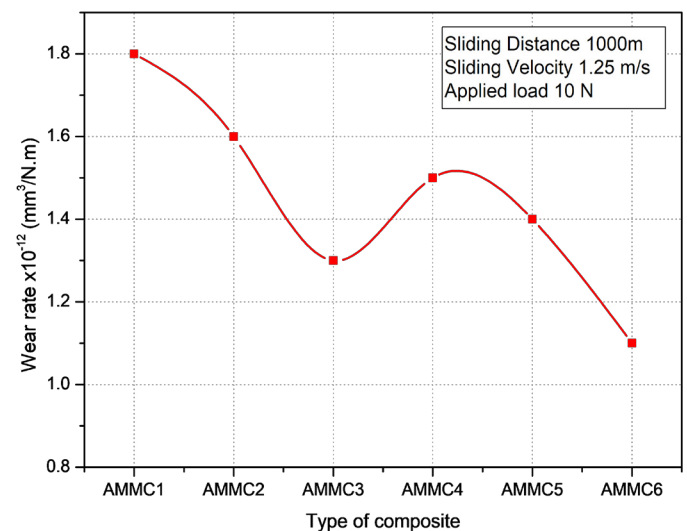Fig. 8. Weight loss of various composite specimens

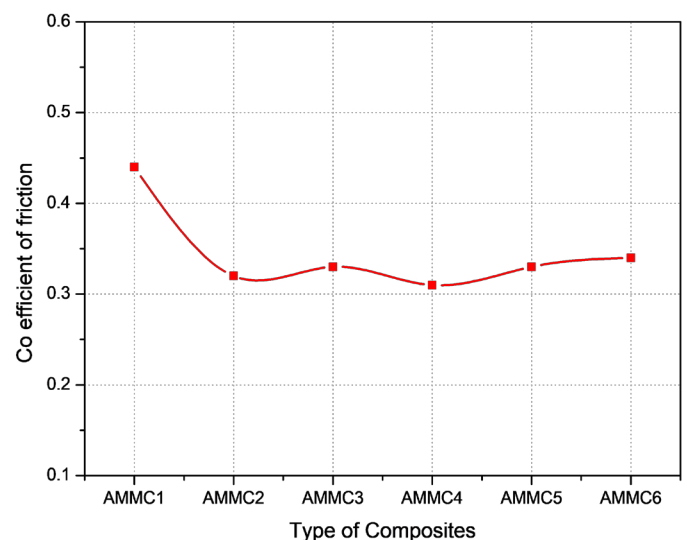Fig. 9. Wear rate of different AMMC specimens

Fig. 10. Co-efficient of friction for different AMMC specimens

3.3. Corrosion behaviour

The corrosion immersion test has studied the corrosion properties of different AMMC composite material grades. After the immersion test, significant corrosion resistance is provided by the NaCl, and the deterioration effect is more when the specimens are immersed in HCl solution. The weight loss plot also shows the impact of nano TiO_2, SiC, and B_4C reinforcement with NaCl and HCl solutions (Fig. 11 and Fig. 12). The corrosion rate is comparatively higher in the HCl solution than the NaCl solution,

and if the concentration of the solution increases, the corrosion rate also increases. Significantly the time plays a significant role in the corrosion rate, and the corrosion rate confirms it is comparatively minimum in 24 hrs duration than the 48 hours in both the solutions (Fig. 13a and Fig. 13b). The Scanning Electron Microscope (SEM) is used to study the corroded AMMC specimens' surface morphology. The result reveals that the specimen with the composition of 1% TiO_2 + 10% SiC + 10% B_4C has corrosion resistance higher than all the other AMMC composition (Fig. 14 to Fig. 15).
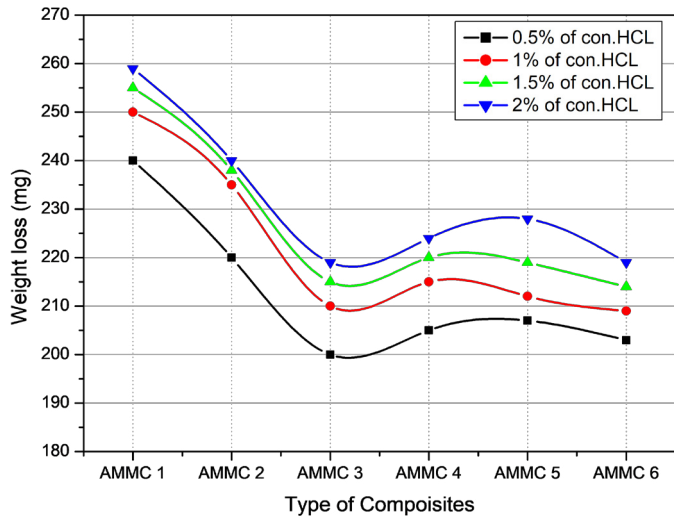

Fig. 11. Weight loss of different composite under various con.of HCL and solution
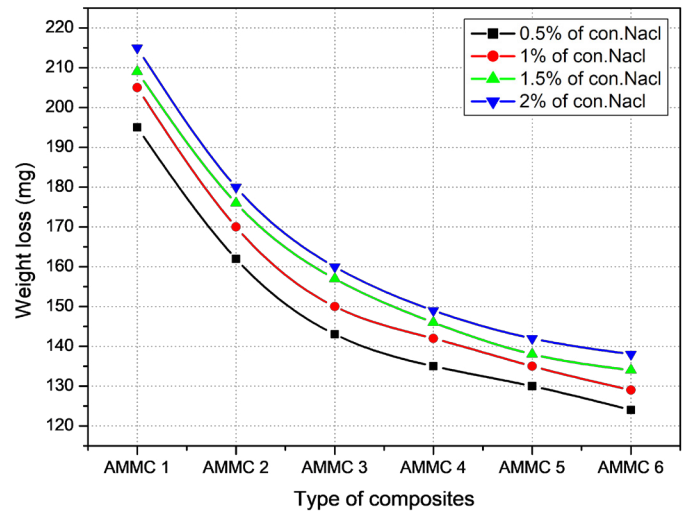

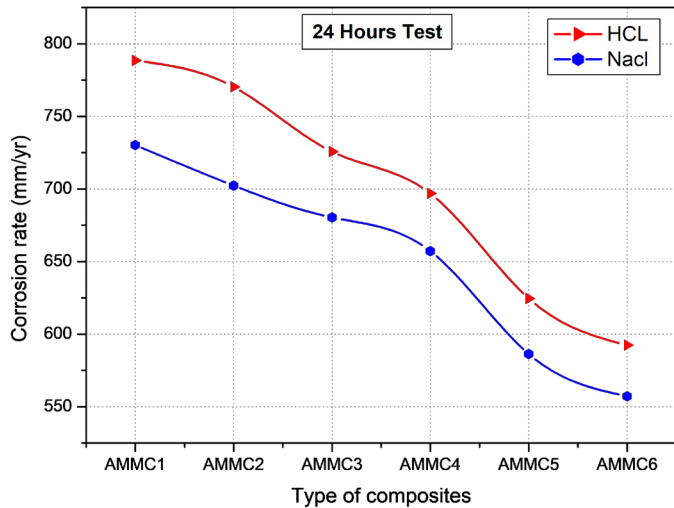Fig. 12. Weight loss of different composite under various con.of NaCl solution

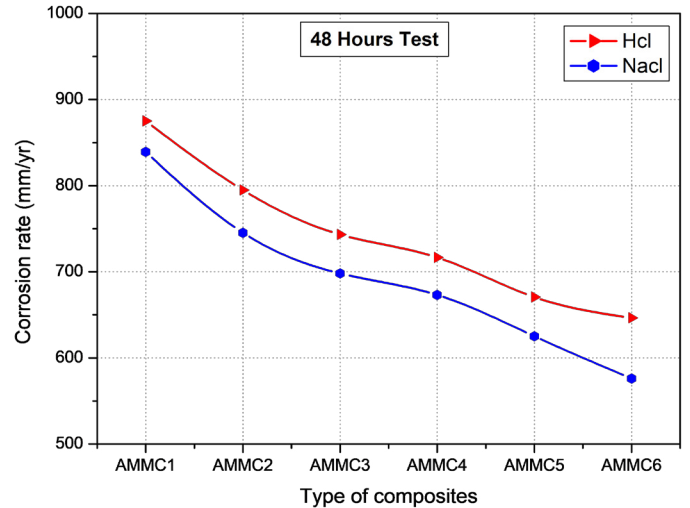Fig. 13a. Corrosion rate of the different composite under 24hrs HCL and NaCl solutions

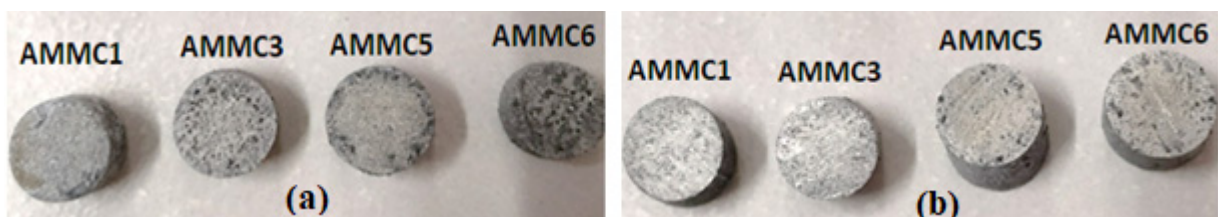Fig. 13b. Corrosion rate of the different composite under 48hrs HCL and NaCl solutions

Fig. 14. Corrosion rate of AMMC specimens after a) 24 and b) 48 hours under 2% NaCl
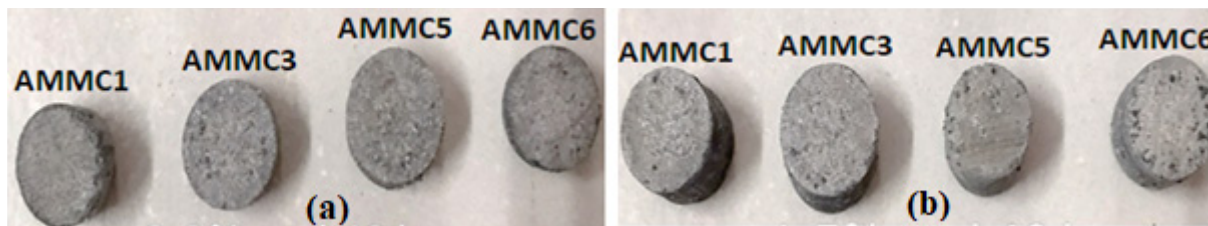
878

Fig. 15. Corrosion rate of AMMC specimens after a) 24 and b) 48 hours under 2% HCl

3.4. Microstructural studies

The worn specimen's microstructure is analyzed by an optical microscope equipped with a high-resolution digital camera. The wear pattern and narrow groove appearance are shown on the surface of the AMMC composite tracks obtained with a regular tear of the material. The nonlinear track with patch tears over the wear surface is observed on the nano TiO_2 reinforced AMMC specimens (Fig. 16). The patch formations are due to the resistance offered by the nanomaterial ingredient of different volume percent.

The AMMC1 specimen's microstructure shows the maximum weight loss compared to the other AMMC specimens. Agglomeration of the nanoparticles is found in several areas due to the stirring speed variations. The addition of nano TiO_2 and micro SIC/B_4C particles is destruction in the worn-out areas as the nano TiO_2 ceramic particles are pinned onto the matrix material and increases the low strain zone area so that minimum material wear is observed. The influence of nano TiO_2 and micro SiC/B_4C particles is offered to resistance to wear. The hard ceramic particles peel off from the matrix material and pitting corrosion occurs (Fig. 17). Dark groove patches' appearance is due to nano and microparticles that tear the material surface from the low strain zone. More uniform tearing of material experienced reveals that the nanoparticle reinforcements resist the free abrasion and encourage the entire strain zone area tearing because of nano TiO_2 particulates.
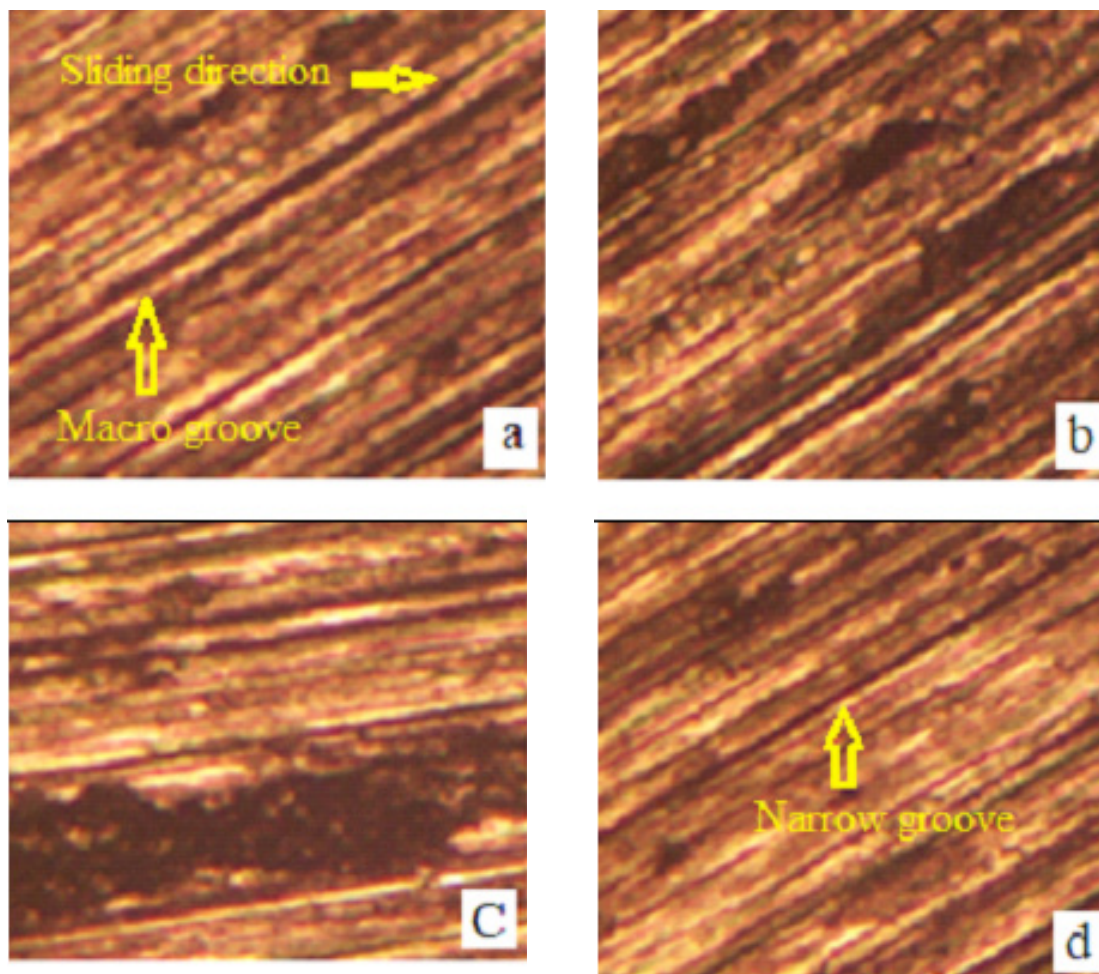

Fig. 16. Micrographs of worn surface of a) AMMC1 b) AMMC3 c) AMMC5 d) AMMC6 composites
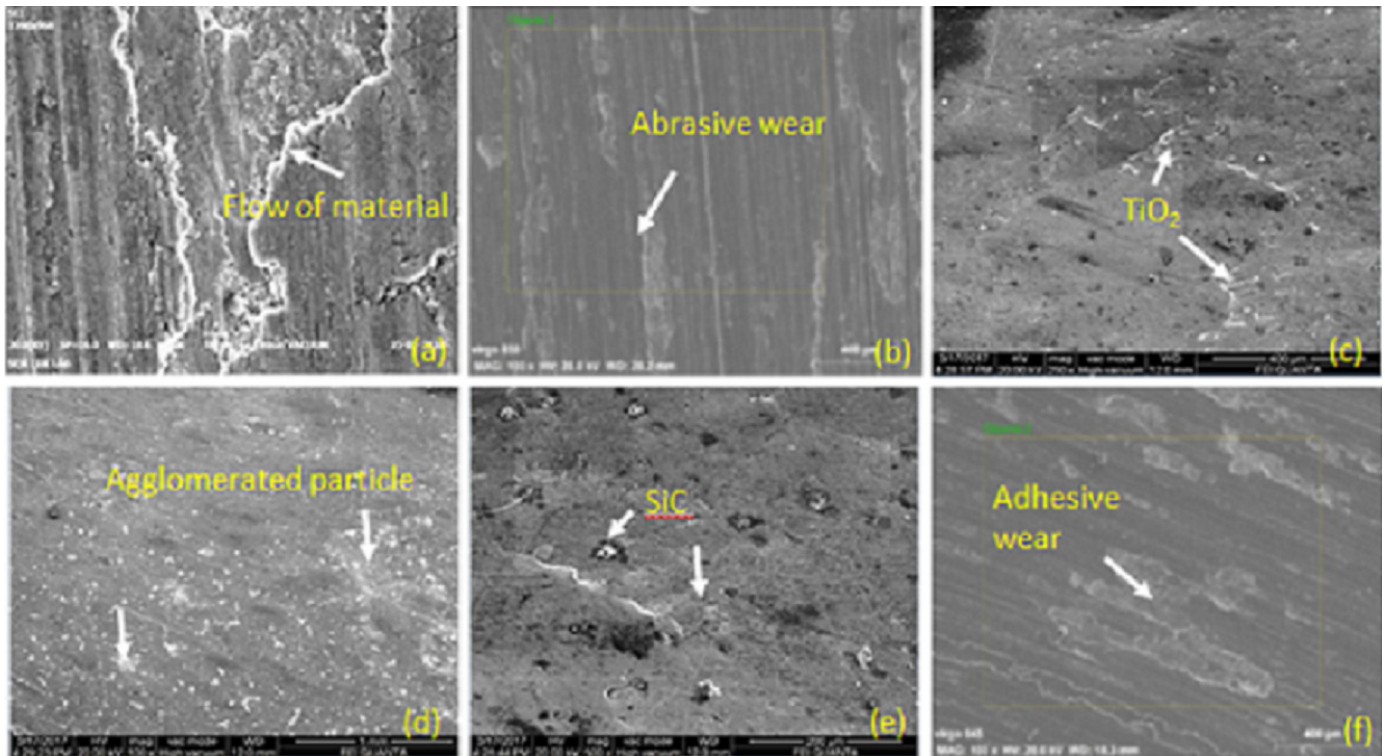
Fig. 17. SEM and EDAX images of a) pure A356 b) 0.5 % nanoTiO$_2$ + A356 c) 1.0 % nano TiO$_2$ + A356 d) 1.5 % nanoTiO$_2$ + A356

4. Conclusion

The following conclusions are revealed based on the test results of the AMMC specimens.

- The tensile strength is enhanced by 9.41% by increasing the nano TiO$_2$ from 0.5% to 1% along with SiC (5% to 10%) in AMMC2 and AMMC3.
- A significant decrease in the impact strength is observed in the AMMC6 specimen, around 63.25% compared to the AMMC1 material.
- The wear resistance is enriched by 38.88% with the maximum reinforcement of 1% TiO$_2$ + 10% SiC + 10% B$_4$C (AMMC6) compared to A356.
- According to the particles' appropriate addition, the introduction of the nano TiO$_2$ particles enhances the resistance towards abrasion and gradual increment in the friction coefficient properties.
- The corrosion rate is reasonably greater in the HCl solution than the NaCl solution, and if the concentration of the solutions increases, the corrosion rate also improved.

REFERENCES

[1] S.N.A. Safri, M.T.H. Sultan, M. Jawaid, K. Jayakrishna, Impact behavior of hybrid composites for structural applications: a review, Comp. Part B Eng. **133**, 112-21 (2017).
DOI: https://doi.org/10.1016/j.Comp Part B.2017.09.008

[2] Ramanathan Arunachalam, Pradeep Kumar Krishnan, Rajaraman Muraliraja. A review on the production of metal matrix composites through stir casting-Furnace design, properties, challenges, and research opportunities, J. Manuf. Proc. **42**, 213-245 (2019).

[3] M. Kok, Production and mechanical properties of Al$_2$O$_3$ particle-reinforced 2024 aluminium alloy composites, J. Mater. Process. Tech. **161**, 381-7 (2005).

[4] A.M.K. Esawi, K. Morsi, A. Sayed, A.A. Gawad, P. Borah, Fabrication and properties of dispersed carbon nanotube-aluminum composites, Mater. Sci. Eng. A. **508** (1), 167-73 (2009).

[5] I. Sridhar, K.R. Narayanan, Processing and characterization of MWCNT reinforced aluminum matrix composites, J. Mater. Sci. **44** (7), 1750-6 (2009).

[6] L. Wang, H. Choi, J.M. Myoung, W. Lee, Mechanical alloying of multi-walled carbon nanotubes and aluminium powders for the preparation of carbon/metal composites, Carbon. **47** 15), 3427-33 (2009).

[7] D.J. Woo, F.C. Heer, L.N. Brewer, J.P. Hooper, S. Osswald, Synthesis of nanodiamond-reinforced aluminum metal matrix composites using cold-spray deposition, Carbon. **86**, 15-25 (2015).

[8] S. Balasivanandha Prabu, L. Karunamoorthy, S. Kathiresan, B. Mohan, Influence of Stirring Speed and Stirring Time on Distribution of Particles in Cast Metal Matrix Composite, J. Mater. Proc. Tech, **171**, 268-273 (2006).

[9] R. Mishra Sheok, R.K. Srivastava. Tribological behaviour of Al-6061/SiC metal matrix composite by Taguchi's techniques, Int. Jour. Scic. Res. Pub. **2** (10), 1-8 (2012).

[10] Jigar Suthar, K.M. Patel. Processing issues, machining, and applications of aluminum metal matrix composites, Mat. Manuf. Proc. **33** (5), 499-527 (2018).

[11] A.S. Vencl, F. Vučetić, B. Bobić, J. Pitel, I. Bobić, Tribological characterization in dry sliding conditions of compocasted hybrid

A356/SiCp/Grp composites with graphite macroparticles. Int Jour Adv Manuf Tech. part of Springer Nature, (2018).

[12] B.K. Prasad, O.P. Modi, Sliding wear response of zinc based alloy as affected by suspended solid lubricant particles in oil lubricant, Tribology - Materials, Surf. & Interf. **2** (2), 84-91 (2008).

[13] H. Mazahery, H. Abdizadeh, R. Baharvandi, Development of high-performance A356/nano-Al_2O_3 composites, Mat. Sci. Engg. A. **518**, 61-64 (2009).

[14] Ali Mazahery, Mohsen Ostad Shabani. Influence of the hard-coated B_4C particulates on wear resistance of Al-Cu alloys, Comp: Part B. **43**, 1302-1308 (2012).

[15] M. Karbalaei Akbari, H.R. Baharvandi, K. Shirvanimoghaddam, Tensile and fracture behavior of nano/micro TiB_2 particle reinforced, Mat. Desn. **66**, 150-161 (2015).

[16] R. Senthil kumar, K. Prabu, G. Rajamurugan, P. Ponnusamy, Comparative analysis of particle size on the mechanical and metallurgical characteristics of Al_2O_3 reinforced sintered and extruded AA2014 nano hybrid composite, Jour. Comp. Mat. **53** (28-29), 4369-4384 (2019).
DOI: https://doi.org/10.1177/0021998319856676

[17] B.K. Prasad, Effects of some solid lubricant particles and their concentration in oil towards controlling wear performance of leaded tin bronze bush, Can. Metal Quar. **51** (2), 210-220 (2012).
DOI: https://doi.org/10.1179/1879139511Y.0000000030

[18] P. Sangaravadivel, G. Rajamurugan, P. Krishnasamy, Significance of tungsten disulfide on the mechanical and machining characteristics of phosphor bronze metal matrix composite, Advanced Composites Letters **29**, 1-13 (2020).
DOI: https://doi.org/10.1177/2633366X20962496

[19] A. Vencl, I. Bobic, S. Arostegui, B. Bobic, A. Marinković, M. Babić, Structural, mechanical and tribological properties of A356 aluminum alloy reinforced with Al2O3, SiC, and SiC + graphite particles. J. All and Comp. **506**, 631-639 (2010).

[20] A. Singh, G. Rajamurugan, K. Prabu, D. Dinesh, Surface modification of aluminium alloy 5083 reinforced with Cr2O3/TiO_2 by friction stir process, SAE Tech. paper, 2019-28-0179, 1-7 (2019).
DOI: https://doi.org/10.4271/2019-28-0179

[21] S. Jaiswal, G. Rajamurugan, P. Krishnasamy, Y. Shaswat, M. Kaushik, Mechanical and Corrosion Behaviour of Al 7075 Composite Reinforced with TiC and Al2O3 Particles, SAE Tech. Paper, 2019-28-0094 (2019).
DOI: https://doi.org/10.4271/2019-28-0094